Article

Discovery Medicine 2026; 38(204): 256–266
https://doi.org/10.24976/Discov.Med.202638204.20

The Effect of Cu/Zn-SOD Overexpression on Uremia-associated Cerebral Hemorrhage

Leping Cheng[1,2], Liangwen Cui[1], Yutao Zha[1], Rui Huang[1], Delong Zhang[2], Min Shao[1,*]

[1]Department of Critical Care Medicine, The First Affiliated Hospital of Anhui Medical University, 230022 Hefei, Anhui, China
[2]Department of Critical Care Medicine, Tongling People's Hospital, 244000 Tongling, Anhui, China
*Correspondence: shaominahaq2021@163.com (Min Shao)
Submitted: 18 August 2025 Revised: 18 December 2025 Accepted: 24 December 2025 Published: 20 January 2026

Background: Cu/Zn-SOD plays a crucial role in uremia combined with cerebral hemorrhage (UCH). However, its specific role and underlying mechanisms in this condition have not been fully elucidated. This study aims to investigate the effects of Cu/Zn-SOD on uremia-associated cerebral hemorrhage and whether the NF-κB pathway is involved.
Methods: Samples were collected from healthy adult subjects and age-matched patients with uremic cerebral hemorrhage, and a UCH mouse model was established. Western blot and RT-qPCR analyses were used to evaluate the levels of Cu/Zn-SOD, apoptosis-related proteins, inflammatory cytokines, oxidative stress markers, and proteins involved in the NF-κB pathway in UCH patients. The brain water content measurement, ELISA, TUNEL, immunofluorescence, and DCFH-DA assays were also performed to assess brain edema, apoptosis, inflammation, and oxidative stress in UCH brain tissue.
Results: Cu/Zn-SOD expression was significantly downregulated in the human serum of UCH patients ($p < 0.001$). Overexpression (OE) of Cu/Zn-SOD alleviated brain edema and inhibited cellular apoptosis in mice ($p < 0.05$), which was reversed by RNAi ($p < 0.05$). Furthermore, OE reduced inflammation and oxidative stress levels in UCH mice ($p < 0.05$), which was reversed by RNAi ($p < 0.05$). Notably, OE suppressed the expression of NF-κB pathway proteins ($p < 0.001$), while the NF-κB agonist reversed the inhibitory effect of OE on NF-κB ($p < 0.001$).
Conclusions: Overexpression of Cu/Zn-SOD alleviates the occurrence of UCH by inhibiting the NF-κB pathway, thereby providing a theoretical reference for Cu/Zn-SOD as a potential target for the prevention and treatment of UCH.

Keywords: Cu/Zn-SOD; overexpression; uremia-associated cerebral hemorrhage

Introduction

Uremia is a clinical syndrome caused by severe renal failure, characterized by the accumulation of toxins in the body, such as urea and creatinine, that are inadequately cleared by the kidneys; this condition is associated with a range of complications [1]. The uremic phase is the terminal stage of chronic renal failure, during which cerebral hemorrhage is a frequent and particularly severe complication [2]. Patients with uremia are susceptible to cerebral hemorrhage, which presents with an acute onset. When cerebral hemorrhage occurs, it is often characterized by a substantial bleeding volume in the brain and marked cerebral oedema, with rapid progression of the condition. The oedema is prone to pressure on the adjacent brain tissues, and the hemorrhage ruptures into the cerebral ventricle, which poses considerable therapeutic challenges, resulting in a very high mortality rate [3]. Furthermore, this disease poses an extremely heavy economic burden on both families and society. The diagnosis of uremia combined with cerebral hemorrhage (UCH) relies on post-onset imaging testing, lacking effective early predictive tools and molecular biomarkers. Once a cerebral hemorrhage occurs, it significantly worsens the patient's prognosis. Therefore, exploring early diagnostic markers and intervention strategies is of great importance for improving prognosis outcomes in UCH.

Cu/Zn-SOD (Copper-zinc superoxide dismutase) functions as a vital antioxidant enzyme, essential for cellular defense against oxidative stress. Cu/Zn-SOD facilitates the conversion of superoxide anions into molecular oxygen (O_2) and hydrogen peroxide (H_2O_2), thereby mitigating potential oxidative damage [4,5]. It plays a protective role in various tissues and can prevent the tissues from oxidative damage [6]. In addition, research demonstrated that Cu/Zn-SOD has the capacity to efficiently scavenge reactive oxygen species (ROS), thereby contributing to the regulation of redox equilibrium in the immune system [7]. However, there is limited understanding of Cu/Zn-SOD's role in UCH and its related mechanisms.

NF-κB serves as a central regulator of gene expression related to immunity, inflammatory pathways, cellular longevity, and growth process [8], and plays an essential role in both normal physiology and disease [9,10]. The most common active form of NF-κB is a heterodimer composed of a p50 or p52 subunit and a p65 subunit, which

provides the transcriptional activation domains required for gene induction [11]. NF-κB has a dual role in apoptosis. The effect of NF-κB on apoptosis depends on the cell type and the signaling environment, and may have both pro-apoptotic and anti-apoptotic functions [12–14]. NF-κB interacts with molecules such as Akt and AP-1 to form a complex regulatory network that governs the cell fate [15]. Previous research has verified that in mice lacking Cu and Zn-SOD, the amount of oxidatively damaged DNA in specific organs increased, and the activity of NF-κB1 protein also rose [16]. However, the specific role of Cu/Zn-SOD in regulating the occurrence of UCH through the NF-κB pathway remains unclear.

In this study, we investigated the expression of Cu/Zn-SOD in patients with UCH. We also analyzed how overexpression and knockdown of Cu/Zn-SOD regulate the NF-κB pathway to affect brain edema, apoptosis, inflammatory response, and oxidative stress in UCH mice.

Methods

Sample Acquisition

The study consists of two groups of human serum samples. Thirty samples from healthy adults were used as the normal group, and thirty samples from patients with UCH were used as the experimental group. Inclusion criteria for patients with UCH: (1) eGFR $<$15 mL/min/1.73 m^2; (2) cerebral hemorrhage foci were detected in the brain parenchyma through CT or MRI scans. Exclusion criteria for patients with UCH: (1) normal renal function (normal eGFR); (2) no high-density hemorrhagic foci observed on plain CT scan of the head; (3) blood creatinine and urea nitrogen levels are within normal range or only slightly elevated. In terms of baseline data, such as gender, age, body mass index, smoking history, alcohol consumption, and other comorbidities, there were no significant differences between the normal group and the UCH group. Human serum specimens were promptly immersed in liquid nitrogen and preserved at –80 °C. All patients provided informed consent to participate in this study. The study was approved by the ethics committee of Tongling People's Hospital (Approval No.2025LW030) and adhered to the Helsinki Declaration.

RT-qPCR

RNA was isolated from serum specimens and subsequently converted into cDNA utilizing a reverse transcription kit (4368813, Thermo Fisher Scientific, Waltham, MA, USA). PCR amplification was performed using the TB Green® Premix Ex Taq™ Kit (RR071A, BIOSCIENCE, Hong Kong, China) on a Real-Time PCR System (480, Roche, Shanghai, China). Relative expression of target genes was quantified by applying the $2^{-\Delta\Delta Ct}$. The primer sequences are listed in Table 1.

Western Blot Analysis

Each blood and brain tissue sample was collected and dissolved in Triton X-100 (HFH10, Thermo Fisher Scientific, Waltham, MA, USA)/glycerol buffer (15514011, Thermo Fisher Scientific, Waltham, MA, USA). The protein concentration in the serum and brain tissue samples was determined using a BCA protein assay kit (23227, Pierce, Rockford, IL, USA), followed by a mixture of an appropriate volume of serum and brain tissue sample with DTT. Then, the mixture was heated at 95–100 °C for 5–10 minutes to ensure complete protein denaturation. The processed samples were subjected to SDS-PAGE to allow for protein separation via electrophoresis. Upon completion of electrophoretic separation, proteins were transferred onto PVDF membranes (88585, Thermo Fisher Scientific, Waltham, MA, USA) to facilitate subsequent immunological detection. To prevent nonspecific binding, the membranes were treated with Tris-buffered saline and 5% nonfat milk, and then the membrane was incubated with the primary antibodies: anti-Cu/Zn-SOD [1: 1000, LM-10216R, LMAI Bio, Shanghai, China], anti-Bax [1:1000, ab32503, Abcam, Cambridge, UK], anti-cleaved caspase 3 [1:5000, ab214430, Abcam, Cambridge, UK], anti-Bcl-2 [1:500, ab194583, Abcam, Cambridge, UK], anti-TNF-a [1:1000, ab66579, Abcam, Cambridge, UK], anti-IL-6 [1:1000, ab324449, Abcam, Cambridge, UK], anti-Nrf2 [1:2000, AF0639, Affinity, MI, USA], anti-Lamin-A [1:5000, ab26300, Abcam, Cambridge, UK], anti-HO-1 [1:1000, AF5393, Affinity, MI, USA], anti-Histone H3 [1:1000, ab1791, Abcam, Cambridge, UK], anti-IκBα [1:1000, 9242, CST, TA, USA], anti-p-IκBα [1:1000, 2859, CST, TA, USA], anti-NF-κB [1:1000, AF5006, Affinity, MI, USA] and anti-β-actin [1:2000, ab8227, Abcam, Cambridge, UK] at room temperature for 3 hours. Subsequently, the membranes were incubated with the secondary antibody (1:10000, ab7090, Abcam, Cambridge, UK) for 1.5 hours. Protein detection was performed using the SuperSignal® West Dura Extended Duration chemiluminescent substrate (34076, Thermo Fisher Scientific, Waltham, MA, USA).

Animal

C57BL/6J mice (12 weeks, 25–30 g, female and male) were obtained from The Jackson Laboratory (Shanghai, China). The animals were housed in groups within standard cages under controlled environmental conditions, including stable temperature and humidity, with a 12-hour light/dark cycle. All animal-related experiments were conducted in accordance with ethical standards outlined in the NIH, ensuring proper care and responsible use of laboratory animals. All experimental protocols of this study were approved by the ethics committee of the Beijing Biocisco Biomedical Technology Co., Ltd. (No: MDL 2024-10-21-01).

Table 1. Sequence of RT-qPCR primers.

Primer names	Forward primer (5′-3′)	Reverse primer (5′-3′)
Cu/Zn-SOD	CCAGTGCAGGGCATCATCAA	CAAGCCAAACGACTTCCAGC
IL-6	CAACGATGATGCACTTGCAGA	TCTCTCTGAAGGACTCTGGCT
TNF-α	ACCTGGCCTCTCTACCTTGT	CCCGTAGGGCGATTACAGTC
HO-1	AGACCGCCTTCCTGCTCAACAT	TCTGACGAAGTGACGCCATCTGT
β-actin	GGGAAATCGTGCCGTGACAT	GCGGCAGTGGCCATCTC

UCH Model and Treatment

A uremia model was established using the method reported previously [17,18]. In the Sham group, only the kidneys were exposed during both surgeries, and the perirenal fat and capsule were separated, followed by suturing. In the other groups, 5/6 nephrectomy (5/6 NPM) was performed. Mice were rendered unconscious through an intraperitoneal administration of 0.05% sodium pentobarbital (Sigma, Santa Clara, CA, USA) and subsequently positioned on the operating platform for the procedure. After preparation of the surgical sets by shaving and disinfection, an approximately 45° oblique incision (0.8–1 cm below the left rib to the inward relative to the longitudinal axis of the body) was made to expose the left kidney. The perirenal fat was separated, and the renal capsule was removed. One-third of the upper and lower poles of the left kidney was excised. Hemostasis was achieved by 10-minute compression with a gelatin sponge (Pfizer, New York, NY, USA), after which the kidney was repositioned, and the incision was sutured. Penicillin (Pfizer, New York, NY, USA) was administered intraperitoneally postoperatively for infection prophylaxis. One week later, an incision was made on the right dorsal side to expose the right kidney, which was then completely removed after ligating the renal pedicle. Thus, approximately 5/6 of the total renal mass was removed across the two surgeries. At this point, the uremia model was established, and uremia was induced after eight weeks. If serum creatinine and urea nitrogen of the uremia rats were 2–3 times higher than those of the normal rats, the modeling of uremia mice was considered successful [19]. Subsequently, a cerebral hemorrhage model was established using a previously reported method [20]. Cerebral hemorrhage surgery: Intracerebral hemorrhage (ICH) was induced by injecting collagenase IV. After injecting 0.05% pentobarbital sodium (Sigma, Santa Clara, CA, USA) into the abdominal cavity of the mice, the mice were stabilized in a stereotaxic apparatus, and a small burr hole was created in the right hemisphere of the skull at coordinates 0.5 mm anterior and 2 mm lateral to the bregma. A fine needle (Boston Scientific, Marlborough, MA, USA) was inserted to a depth of 3 mm, targeting the striatum. Subsequently, 400 nL of phosphate-buffered saline supplemented with 0.075 U of collagenase IV was delivered using a microinjection system (Nanoject III, Drummond Scientific, USA). After the injection, the needle was left in place for 5 minutes. The needle was then withdrawn, the hole was sealed with bone wax, and the incision was sutured; in the ICH group, the ICH model was established using the above procedure. In the Sham group, the procedure was performed without collagenase IV injection. The higher water content in the brains of the mice compared to the sham group indicates that the cerebral hemorrhage model has been successfully established. Cervical dislocation was used as the method of euthanasia for all the animals used in this research.

The mice were randomized into six groups (n = 6): (1) Sham: Untreated sham group; (2) UCH: mice with both uremia and ICH models established; (3) Overexpression (OE)-Cu/Zn-SOD: mice intravenously injected with a Cu/Zn-SOD overexpression plasmid 48 hours after UCH model establishment; (4) si-Cu/Zn-SOD: mice intravenously injected with a Cu/Zn-SOD knockdown plasmid 48 hours after UCH model establishment; (5) OE-Cu/Zn-SOD + LPS: mice in the OE-Cu/Zn-SOD group additionally injected with lipopolysaccharide (LPS); (6) si-Cu/Zn-SOD + LPS: mice in the si-Cu/Zn-SOD group additionally injected with LPS.

Transfection

The RNAi (siRNA) and overexpression (OE) of Cu/Zn-SOD were designed and synthesized by SHANGYA (Zhejiang, China), using si-NC and OE-NC as controls. The primer for si-Cu/Zn-SOD was forward 5′-GGAAATGAAGAAAGTACAA-3′. The primer for si-NC was forward 5′-AGAGTAAGAGAAGATAACA-3′. The primers for Ad-Cu/Zn-SOD were forward 5′-ATGGCGATGAAAGCGGTGTG-3′ and reverse 5′-CTGCGCAATCCCAATCACTCCAC-3′. The primers for Ad-NC were forward 5′-CAGTGCTGCAATGATACCGC-3′ and reverse 5′-TCCTTGAGAGTTTTCGCCCC-3′. They were injected intravenously into mice, and brain samples were collected after 48 hours. Each experimental group was repeated three times.

Brain Water Content

Brain water content for each group was measured using the wet-dry method. C57BL/6J mice weighing 25 to 30 g were intraperitoneally injected with 40 mg/kg of 1% sodium pentobarbital for anesthesia. After anesthesia, the cerebral hemisphere was removed within approximately 1 minute and immediately weighed to determine the wet weight (WW). The tissue was then dried at 100 °C for 2

days to obtain the dry weight (DW). Brain water content was used as an indicator of cerebral edema.

TUNEL Assay

TUNEL staining was performed using a BrdU-Red TUNEL assay kit (ab66110, Abcam, Cambridge, UK) to identify apoptotic cells. Tissue sections were permeabilized in 10% Triton for 15 minutes and stained for 1 hour. Subsequently, each section was stained with DAPI (62,248, Thermo Scientific, Waltham, MA, USA) for 15 minutes. Finally, the sections were observed and imaged using a fluorescence microscope (AX70, Olympus, Center Valley, PA, USA).

ELISA

A 20 µL mouse plasma sample was mixed with 200 µL of the working solution for the assay. TNF-α, IL-6, glutathione (GSH), and catalase (CAT) levels were measured using ELISA kits (TNF-α, PT513; IL-6, PI326; Beyotime, Shanghai, China; GSH, KCW20064, KECHENGWEI, Shanghai, China; CAT, EN-XS91755, BIOSCIENCES, Shanghai, China).

Immunofluorescence

Mice were euthanized, and their brain tissue samples were fixed overnight in 4% PFA, then embedded in optimal cutting temperature compound (OCT) for preparation of frozen sections. Continuous brain sections, 6 µm thick, were prepared using a cryostat. The sections were incubated overnight with the primary antibody IL-6 (ab290735, Abcam, Cambridge, UK). They were then incubated with the secondary antibody (1:100, ab150077, Abcam, Cambridge, UK) and stained with DAPI for 15 minutes. The DAPI staining solution was removed, and the sections were washed 2–3 times using PBS (14190136, Thermo Fisher Scientific, Waltham, MA, USA). The cells were examined using a confocal microscope (FV3000, OLYMPUS, Tokyo, Japan).

ROS

ROS levels were detected using the DCFH-DA probe (S0035S, Beyotime Biotechnology Co., Ltd., Shanghai, China). The brain tissue was mechanically cut into tiny tissue blocks, and then digested with trypsin. After gentle pipetting, the cells were prepared into a single-cell suspension. The cells were inoculated onto petri dishes and cultured in DMEM medium (11965092, Life Technologies, Carlsbad, CA, USA) supplemented with 10% FBS (16000044, Thermo Fisher Scientific, Waltham, MA, USA) under conditions of 35 °C and 10% CO_2. Before the experiment, the cell counts in each group were adjusted to be the same. The DCFH-DA fluorescent probe was prepared by diluting it 1:1000 in a serum-free medium (N6040-1L, Solarbio, Beijing, China). A volume of 1 mL from this diluted mixture was introduced into each well, followed by a 30-minute incubation period. Upon completion of incubation, the cells underwent two washes with a serum-free medium. Intracellular staining intensity was then examined with a fluorescence microscope (AX70, Olympus, Center Valley, PA, USA), and mean fluorescence intensity was calculated using image J (version 1.2, NIH, Bethesda, MD, USA).

Statistical Analysis

Each experiment was performed in triplicate in this study, and the results are presented as means ± SD. Statistical analysis was performed using GraphPad Prism 7 software (GraphPad Software, La Jolla, CA, USA). For comparisons involving more than two groups, one-way ANOVA followed by Tukey's post hoc analysis was performed. The *t*-test was applied to assess differences between two groups. Statistical significance was defined as a *p*-value below 0.05.

Results

Cu/Zn-SOD Is Downregulated in UCH

To determine the expression pattern of Cu/Zn-SOD in UCH, Cu/Zn-SOD expression levels in the serum of patients with UCH was assessed using RT-qPCR and Western blot analyses. Compared to the normal group, the mRNA expression of Cu/Zn-SOD was significantly downregulated in the UCH group ($p < 0.001$) (Fig. 1A). Similarly, the protein expression of Cu/Zn-SOD was also markedly reduced in the UCH group compared to the normal group ($p < 0.001$) (Fig. 1B). These findings indicate that the occurrence of UCH may be associated with lower expression of Cu/Zn-SOD.

Overexpression of Cu/Zn-SOD Alleviates Brain Edema and Inhibits Apoptosis in Mice

RT-qPCR was used to verify the efficiency of Cu/Zn-SOD overexpression and knockdown. The results showed that the construction of Cu/Zn-SOD overexpression and knockdown was successful ($p < 0.001$) (Fig. 2A). To verify whether overexpression of Cu/Zn-SOD alleviates brain edema and inhibits apoptosis in mice with UCH, a mouse model of UCH was established, and Cu/Zn-SOD overexpression and knockdown plasmids were constructed. Based on the UCH model, mice were intravenously injected with either the OE plasmid or the RNAi plasmid. Brain water content was assessed in each group 3 days after surgery. The results showed that the UCH model group had significantly higher brain water content compared to the Sham group ($p < 0.01$) (Fig. 2B). The RNAi group further increased brain water content, while the OE group reduced it ($p < 0.05$) (Fig. 2B). In addition, the number of TUNEL-positive cells was significantly increased in the UCH group compared to the Sham group ($p < 0.001$) (Fig. 2C). Compared to the UCH group, RNAi further increased the number of TUNEL-positive cells, whereas OE reversed this ef-

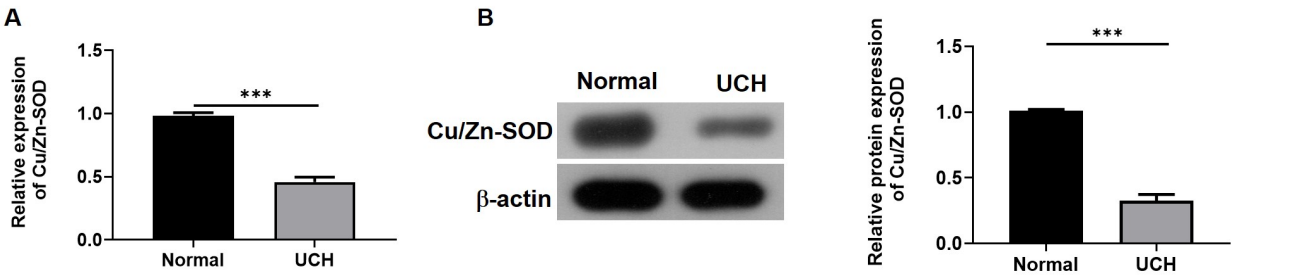

Fig. 1. Cu/Zn-SOD levels in the serum of human patients with UCH and without. (A) RT-qPCR and (B) Western blot analyses were used to measure the mRNA and protein expression of Cu/Zn-SOD in the serum of 30 patients with UCH and without. n = 30. ***$p <$ 0.001 vs Normal group. UCH, uremia combined with cerebral hemorrhage.

fect ($p < 0.001$) (Fig. 2C). Western blot analysis showed that OE reduced the levels of apoptosis proteins Cleaved caspase-3 and Bax in the brain tissues of UCH mice, while increased the levels of the protein Bcl-2 ($p < 0.05$) (Fig. 2D). In contrast, RNAi exhibited the opposite trend ($p < 0.05$) (Fig. 2D). Hence, the results demonstrate that overexpression of Cu/Zn-SOD ameliorates brain edema and apoptosis in UCH mice.

Overexpression of Cu/Zn-SOD Alleviates the Inflammatory Response in UCH Mice

To further analyze the effect of Cu/Zn-SOD overexpression on inflammation in a uremic intracerebral hemorrhage mouse model, the levels of TNF-α and IL-6 in brain tissues and serum were examined. Western blot results showed that the protein levels of inflammatory factors TNF-α and IL-6 were significantly increased in the UCH group compared with the Sham group ($p < 0.05$) (Fig. 3A). Compared with the UCH group, the OE group reduced the expression level of pro-inflammatory proteins, whereas the RNAi group increased it ($p < 0.05$) (Fig. 3A). ELISA results demonstrated that the levels of inflammatory factors TNF-α and IL-6 in the UCH group were significantly higher than those in the sham group ($p < 0.01$) (Fig. 3B). Notably, RNAi exacerbated the inflammatory response in UCH mice, while OE treatment alleviated it ($p <$ 0.05) (Fig. 3B). Immunofluorescence results of mouse brain tissue further supported these findings (Fig. 3C). Overall, these findings indicate that overexpression of Cu/Zn-SOD alleviates the inflammatory response in uremic intracerebral hemorrhage mice.

Overexpression of Cu/Zn-SOD Improves Oxidative Stress and Reduces ROS Accumulation in UCH Mice

GSH and CAT are two important antioxidant enzymes in the body, playing a significant role in oxidative stress. The levels of GSH and CAT in the UCH mice were markedly lower than those in the Sham group ($p < 0.01$) (Fig. 4A). In contrast with the UCH group, the levels of GSH and CAT in serum were elevated remarkably after OE treatment, whereas they were reduced by RNAi ($p < 0.01$). In addition, the protein expression levels of Nrf2 and HO-1 were higher in the UCH group compared to the Sham group ($p < 0.05$). OE treatment increased the levels of Nrf2 and HO-1 proteins in UCH mice, which was reversed by RNAi ($p < 0.05$) (Fig. 4B). Notably, the UCH model increased ROS accumulation in mice. RNAi further promoted ROS production, whereas OE reduced ROS accumulation ($p <$ 0.05) (Fig. 4C). Overall, overexpression of Cu/Zn-SOD improves oxidative stress and reduces ROS accumulation in UCH mice.

Overexpression of Cu/Zn-SOD Alleviates Inflammation and Oxidative Stress in UCH Mice by Inhibiting NF-κB

The NF-κB pathway plays a significant role in the inflammatory response and cell apoptosis after cerebral hemorrhage [21,22]. To determine whether Cu/Zn-SOD alleviates inflammation and oxidative stress in UCH mice through regulation of NF-κB, we used the NF-κB agonist LPS to simulate the effects of Cu/Zn-SOD overexpression and knockdown on IκBα and NF-κB-p65 activity. The results showed that IκBα and NF-κB-p65 activity was elevated in the UCH group compared to the sham group (p < 0.05) (Fig. 5A). Compared to the UCH group, IκBα and NF-κB-p65 protein levels were significantly downregulated in the OE group and upregulated by RNAi ($p <$ 0.05) (Fig. 5A). IκBα and NF-κB-p65 activity was significantly increased in OE-Cu/Zn-SOD/si-Cu/Zn-SOD groups exposed to LPS ($p < 0.05$) (Fig. 5A). We also evaluated the effect of LPS on the expression of inflammatory cytokines and oxidative stress markers. Compared with the UCH group, the mRNA expression levels of TNF-α and IL-6 in the OE-Cu/Zn-SOD group were significantly downregulated, while the mRNA level of HO-1 was significantly upregulated ($p < 0.05$) (Fig. 5B,C). However, the si-Cu/Zn-SOD group showed the opposite trend ($p < 0.05$) (Fig. 5B,C). Compared with the OE-Cu/Zn-SOD group, the mRNA expression levels of TNF-α and IL-6 in the OE-Cu/Zn-SOD+LPS group were significantly increased, while the mRNA level of HO-1 was significantly decreased ($p < 0.05$) (Fig. 5B,C). In summary, inhibition of NF-κB is

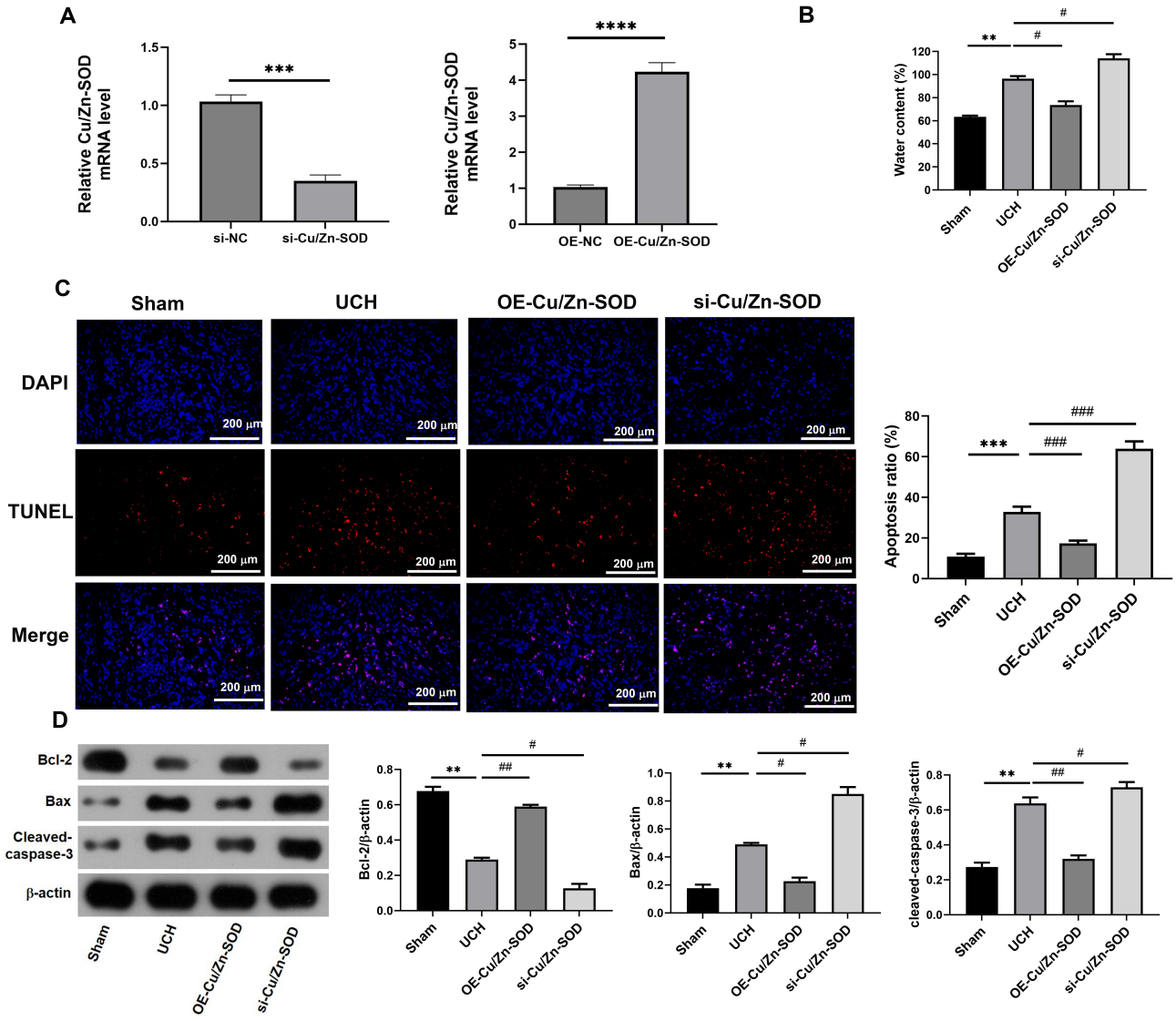

Fig. 2. The effects of Cu/Zn-SOD on brain edema and apoptosis in mice. (A) RT-qPCR verified the effect of RNAi or OE on the relative expression of Cu/Zn-SOD. (B) Brain water content of mice on postoperative day 3. (C) Brain tissue samples were collected on postoperative day 3 for TUNEL staining. (D) Western blotting was used to detect the expression of apoptosis-related genes in mouse brain tissue on postoperative day 3. n = 6. $^{**}p < 0.01$, $^{***}p < 0.001$, $^{****}p < 0.0001$ vs Sham group or si/OE-NC group; $\#p < 0.05$, $\#\#p < 0.01$, $\#\#\#p < 0.001$ vs UCH group.

crucial in UCH, suggesting that overexpression of Cu/Zn-SOD alleviates inflammation and oxidative stress in UCH mice by suppressing NF-κB.

Discussion

The occurrence of cerebrovascular accidents in uremic patients is one of the common critical emergencies in clinical practice, with an extremely poor prognosis, leading to high rates of mortality and disability [23,24]. Cerebral hemorrhage in uremic patients is characterized by sudden onset and high mortality. Diagnosis depends primarily on imaging testing [25,26], and there are relatively few clinical assessment methods and markers. Therefore, a molecular marker for early prediction would help improve prognosis and enhance patients' quality of life, and be of great significance both clinically and socially.

In this study, we conducted a preliminary investigation into the role of Cu/Zn-SOD in patients with UCH. The results showed that, compared to healthy individuals, the expression of Cu/Zn-SOD in the serum of patients with UCH was downregulated, indicating that it is a significant risk factor for patients with UCH. To further investigate the effect of Cu/Zn-SOD on uremic patients with cerebral hemorrhage, we established a mouse model with UCH. It was subsequently observed that OE reduced the occurrence of brain edema in the mice. In addition, TUNEL staining analysis was performed on the brain tissue of mice with UCH.

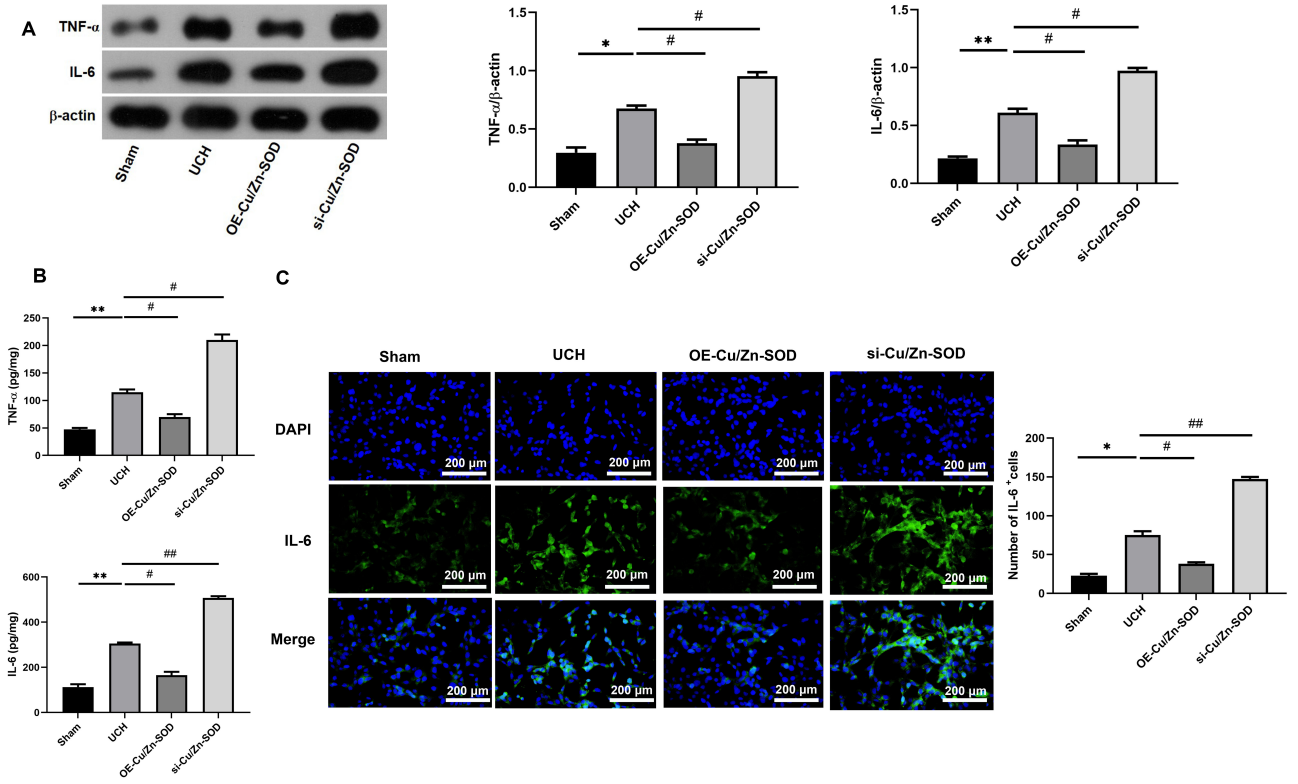

Fig. 3. The effect of Cu/Zn-SOD on inflammation in uremic ICH mice. (A) Western blotting was used to detect the expression of inflammatory factors in brain tissue on postoperative day 3. (B) ELISA was performed to assess the inflammatory levels in mouse serum on postoperative day 3. (C) Immunofluorescence was used to observe IL-6 expression. n = 6. *$p < 0.05$, **$p < 0.01$ vs Sham group; #$p < 0.05$, ##$p < 0.01$ vs UCH group.

The results showed that OE significantly reduced the number of apoptotic cells in the brain tissue, as evidenced by the TUNEL staining results. Cleaved caspase-3, Bax, and Bcl-2 are well known in various diseases, including cerebral hemorrhage, for their roles in regulating cell death and survival [27]. Bcl-2 functions to inhibit apoptosis, whereas Bax acts as a promoter of programmed cell death; both play critical roles in regulating this balance. In addition, caspase-3, an essential protease, is closely associated with the final stages of apoptosis. Zhang *et al.* [28] found that cylindrospermopsin impairs vascular smooth muscle cells through P53-mediated apoptosis caused by ROS overproduction, which is consistent with our study, showing decreased expression of Bcl-2 in UCH mice, along with increased levels of cleaved caspase-3 and Bax proteins. Notably, in this study, overexpression of Cu/Zn-SOD can reverse the expression of these proteins.

In uremic patients, the accumulation of uremic toxins promotes a chronic inflammatory response, which damages vascular endothelial cells and leads to the continuous production of free radicals. These radicals contribute directly or indirectly to cell death. Additionally, uremia can exacerbate the level of microinflammatory responses and upregulate the expression of pro-inflammatory cytokines, key drivers in the pathophysiological mechanism of vascular smooth muscle cell injury [29]. Previous studies have found that during cerebral hemorrhage, the central nervous system activates the body's inflammatory response, resulting from brain cell damage, producing a large amount of inflammatory cytokines such as TNF-α and IL-6, indicating that the secretion and expression of pro-inflammatory factors are positively correlated with brain injury [30,31]. The results are consistent with the findings of this study, as the levels of inflammatory factors TNF-α and IL-6 were significantly increased in the UCH group. The OE-Cu/Zn-SOD reduced the expression of pro-inflammatory proteins, whereas the RNAi group increased it.

Under normal physiological conditions, various antioxidant enzymes are produced in the body to continuously eliminate intracellular ROS and free radicals, thereby maintaining a dynamic balance between oxidative and antioxidative processes. When this balance is disrupted, the formation of oxygen-free radicals is promoted, leading to oxidative stress, cellular damage, and necrosis through cell degeneration [32,33]. Emerging evidence suggests that when the dynamic balance between the rate of superoxide production and the expression level of copper-zinc SOD is disrupted, the effects of oxidative stress can damage en-

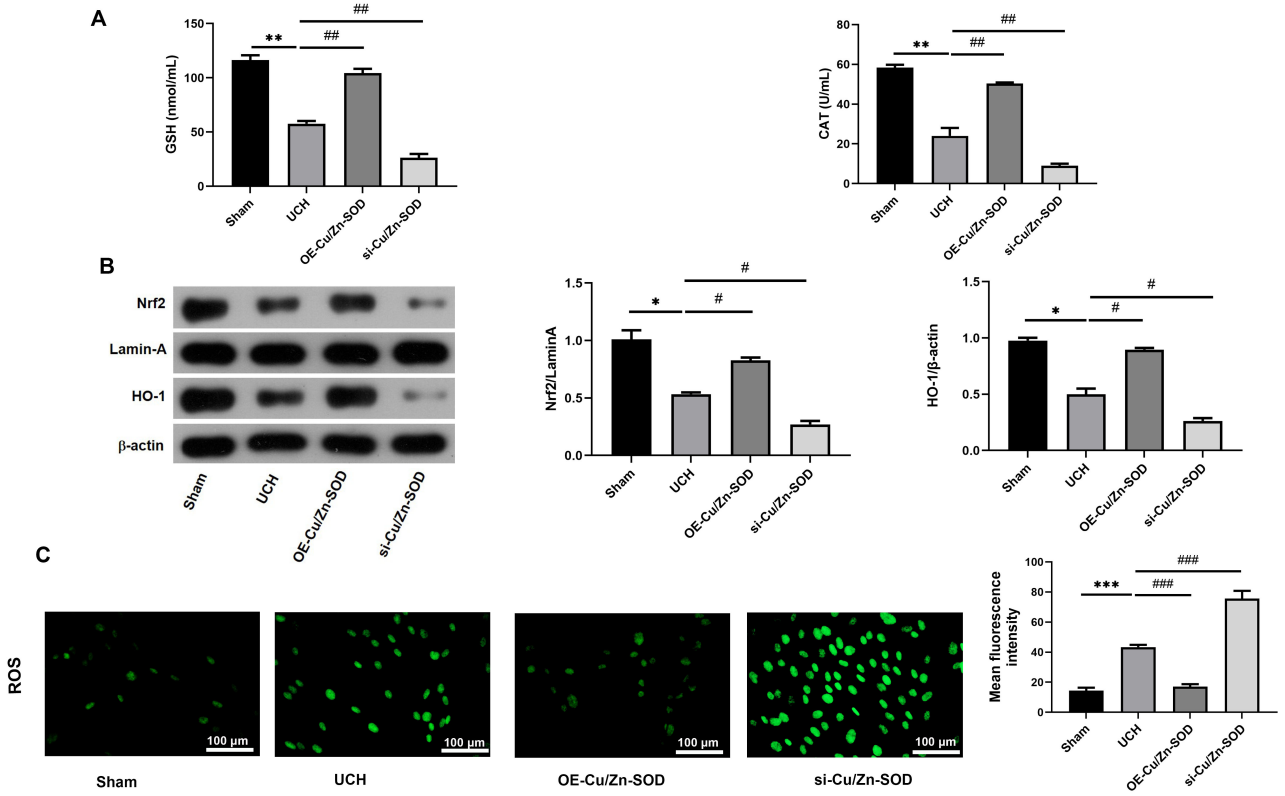

Fig. 4. Effects of Cu/Zn-SOD on oxidative stress and ROS levels in mice with UCH. (A) ELISA was used to assess oxidative stress levels in mouse serum on postoperative day 3. (B) Western blotting was performed to detect the expression of oxidative stress-related factors in brain tissue on postoperative day 3. (C) The ROS levels in mouse brain cells were measured using the DCFH-DA probe. n = 6. *$p < 0.05$, **$p < 0.01$, ***$p < 0.001$ vs Sham group; #$p < 0.05$, ##$p < 0.01$, ###$p < 0.001$ vs UCH group.

dothelial cells, cause capillary sclerosis, increase vascular fragility, and further elevate the risk of hemorrhage [34,35]. Previous study proposed that Cu/Zn-SOD is an antioxidant metalloenzyme present in organisms and plays a crucial role in maintaining the balance between oxidation and antioxidation in the body [36]. It is worth noting that the effect of Cu/Zn-SOD on oxidative stress in the UCH mouse model has not yet been reported. This study shows that the levels of GSH and CAT in the serum were significantly increased after OE intervention compared to the UCH group. OE treatment reduced oxidative stress in UCH mice. Nrf2 is a transcription factor responsible for regulating the synthesis of antioxidants during oxidative stress [37]. In addition, HO-1 is a major target protein of Nrf2 [38]. Research has shown that dimethyl fumarate activates the HO-1/Nrf2 pathway to alleviate oxidative stress-induced acute kidney injury following brain injury [39]. Duan *et al*. [40] found that curcumin restrains oxidative stress after intracerebral hemorrhage in rat by activating the Nrf2/HO-1 pathway. In this study, the protein expression of Nrf2 and HO-1 was significantly increased after OE intervention, which improved the oxidative stress condition in UCH mice. Oxidative stress consists of reactive ROS and antioxidant systems such as SOD. When ROS are in excess or antioxidant systems are insufficient, oxidative stress occurs, ultimately leading to biomolecule damage [41,42]. However, there are fewer studies related to ROS and cerebral hemorrhage complicated by uremia. We used a DCFH-DA probe to detect intracellular ROS levels and assessed the expression of pro-inflammatory factors by flow cytometry. Our study results suggest that OE ameliorates oxidative stress and reduces ROS accumulation in UCH mice.

UCH involves multiple signaling pathways, including NF-κB pathway, NLRP3 inflammatory vesicle pathway, Nrf2/ARE pathway, and PI3K/AKT pathway [43–45]. Although it has been shown that the NF-κB pathway plays a role in human UCH [46], whether Cu/Zn-SOD ameliorates injury in UCH by affecting the NF-κB signaling pathway is unclear. The present study indicated that OE alleviated inflammatory responses and oxidative stress in UCH mice by inhibiting NF-κB, which is consistent with previous studies [47]. To further clarify whether the NF-κB pathway is involved in alleviating the inflammatory response and oxidative stress in UCH mice, we analyzed the role of the NF-κB agonist LPS in mimicking the effects of RNAi and OE on NF-κB activity, and also assessed the effects of LPS on the expression of inflammatory factors and oxidative stress markers. The results reveal that OE alleviates inflammatory responses and oxidative stress in UCH mice by inhibiting NF-κB.

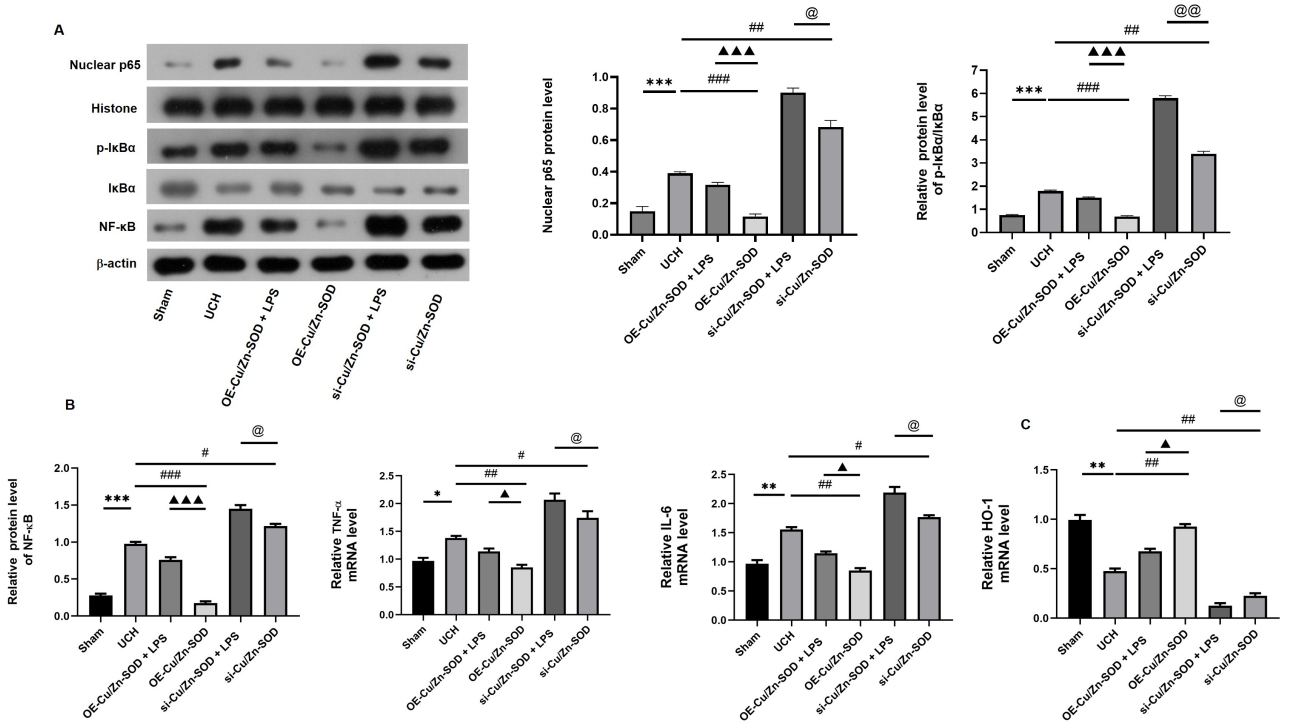

Fig. 5. The effect of Cu/Zn-SOD on inflammation and oxidative stress in UCH mice through the regulation of NF-κB. (A) Western blot analysis was used to assess the protein expression of nuclear NF-κB p65, cytoplasmic IκBα and NF-κB p65 in mouse brain tissue on postoperative day 3. The mRNA expression levels of (B) IL-6, TNF-α, and (C) HO-1 in brain tissue of mice on postoperative day 3. n = 6. *$p < 0.05$, **$p < 0.01$, ***$p < 0.001$ vs Sham group; #$p < 0.05$, ##$p < 0.01$, ###$p < 0.001$ vs UCH group; ▲$p < 0.05$, ▲▲▲$p < 0.001$ vs OE group; @ $p < 0.05$, @@ $p < 0.01$ vs si-Cu/Zn-SOD group.

In conclusion, this study was the first to confirm that Cu/Zn-SOD is downregulated in the serum of UCH patients. *In vivo* experiments demonstrated that overexpression of Cu/Zn-SOD in the UCH mouse model alleviated inflammatory responses and oxidative stress by inhibiting the NF-κB pathway. The results of this study enhanced our understanding of the role of Cu/Zn-SOD in clinical cases of uremic cerebral hemorrhage, providing new theoretical support for the clinical prevention and treatment of uremic patients with cerebral hemorrhage.

Although the results of this study provide new insights into the clinical prevention and treatment of UCH, there are still some limitations. Firstly, since the clinical samples used for detection are relatively small, future research should increase the sample size to verify these results. Secondly, as a preliminary study, the limited number of animals included constrains the statistical power, generalizability and reliability of the research results. Therefore, future studies should employ larger sample sizes. Finally, while the study investigated the levels of Cu/Zn-SOD in UCH patients, its role in the animal model of UCH, and the involvement of the NF-κB pathway, more comprehensive mechanistic research, such as *in vitro* cell experiments, is still needed.

Conclusions

Overexpression of Cu/Zn-SOD alleviates the progression of UCH by inhibiting the NF-κB pathway. Cu/Zn-SOD may serve as a new target and novel approach for the prevention and treatment of UCH, offering effective strategies and new insights for clinical practice.

Availability of Data and Materials

The data used to support the findings of this study are available from the corresponding author upon request.

Author Contributions

LPC and MS designed the research study and wrote the first draft. LWC and YTZ performed the research. RH and DLZ analyzed the data. All authors contributed to important editorial changes in the manuscript. All authors read and approved the final manuscript. All authors have participated sufficiently in the work and agreed to be accountable for all aspects of the work.

Ethics Approval and Consent to Participate

All patients provided informed consent to participate in this study. The study was approved by the ethics committee of Tongling People's Hospital (Approval No.2025LW030) and adhered to the Helsinki Declaration. All experimental protocols of this study were approved by the animal ethics committee of the Beijing Biocisco Biomedical Technology Co., Ltd. (No: MDL 2024-10-21-01).

Acknowledgment

Not applicable.

Funding

This research received no external funding.

Conflict of Interest

The authors declare no conflict of interest.

References

[1] Tonelli M, Karumanchi SA, Thadhani R. Epidemiology and Mechanisms of Uremia-Related Cardiovascular Disease. Circulation. 2016; 133: 518–536. https://doi.org/10.1161/CIRCULATIONAHA.115.018713.

[2] Cordonnier C, Demchuk A, Ziai W, Anderson CS. Intracerebral haemorrhage: Current approaches to acute management. Lancet (London, England). 2018; 392: 1257–1268. https://doi.org/10.1016/S0140-6736(18)31878-6.

[3] Balami JS, Buchan AM. Complications of intracerebral haemorrhage. The Lancet. Neurology. 2012; 11: 101–118. https://doi.org/10.1016/S1474-4422(11)70264-2.

[4] Wang X, Zhang H, Gao Y, Zhang W. Characterization of Cu/Zn-SOD enzyme activities and gene expression in soybean under low nitrogen stress. Journal of the Science of Food and Agriculture. 2016; 96: 2692–2697. https://doi.org/10.1002/jsfa.7387.

[5] Liu H, He J, Chi C, Gu Y. Identification and analysis of icCu/Zn-SOD, Mn-SOD and ecCu/Zn-SOD in superoxide dismutase multigene family of Pseudosciaena crocea. Fish & Shellfish Immunology. 2015; 43: 491–501. https://doi.org/10.1016/j.fsi.2015.01.032.

[6] Lewandowski Ł, Kepinska M, Milnerowicz H. The copper-zinc superoxide dismutase activity in selected diseases. European Journal of Clinical Investigation. 2019; 49: e13036. https://doi.org/10.1111/eci.13036.

[7] Lu X, Wang C, Liu B. The role of Cu/Zn-SOD and Mn-SOD in the immune response to oxidative stress and pathogen challenge in the clam Meretrix meretrix. Fish & Shellfish Immunology. 2015; 42: 58–65. https://doi.org/10.1016/j.fsi.2014.10.027.

[8] Tak PP, Firestein GS. NF-kappaB: A key role in inflammatory diseases. The Journal of Clinical Investigation. 2001; 107: 7–11. https://doi.org/10.1172/JCI11830.

[9] Hayden MS, Ghosh S. NF-κB in immunobiology. Cell Research. 2011; 21: 223–244. https://doi.org/10.1038/cr.2011.13.

[10] Yu H, Lin L, Zhang Z, Zhang H, Hu H. Targeting NF-κB pathway for the therapy of diseases: Mechanism and clinical study. Signal Transduction and Targeted Therapy. 2020; 5: 209. https://doi.org/10.1038/s41392-020-00312-6.

[11] Park MH, Hong JT. Roles of NF-κB in Cancer and Inflammatory Diseases and Their Therapeutic Approaches. Cells. 2016; 5: 15. https://doi.org/10.3390/cells5020015.

[12] Wang CY, Guttridge, Mayo MW, Baldwin Jr As. NF-κB Induces Expression of the Bcl–2 Homologue A1/Bfl–1 To Preferentially Suppress Chemotherapy–Induced Apoptosis. Molecular and Cellular Biology. 1999; 19: 5923-5929. https://doi.org/10.1128/MCB.19.9.5923.

[13] Karin M, Lin, A. NF-κB at the crossroads of life and death. Nature immunology. 2002; 3: 221-227. https://doi.org/10.1038/ni0302-221.

[14] Radhakrishnan S, Kamalakaran S. Pro–apoptotic role of NF–κB: Implications for cancer therapy. Biochimica et Biophysica Acta. 2006; 1766: 53-62. https://doi.org/10.1016/j.bbcan.2006.02.001.

[15] Giridharan S, Srinivasan M. Mechanisms of NF-κB p65 and strategies for therapeutic manipulation. Journal of Inflammation Research. 2018; 11: 407–419. https://doi.org/10.2147/JIR.S140188.

[16] Siomek A, Brzoska K, Sochanowicz B, Gackowski D, Rozalski R, Foksinski M, *et al*. Cu,Zn-superoxide dismutase deficiency in mice leads to organ-specific increase in oxidatively damaged DNA and NF-κB1 protein activity. Acta Biochimica Polonica. 2010; 57: 577–583.

[17] Leenders NHJ, Bos C, Hoekstra T, Schurgers LJ, Vervloet MG, Hoenderop JGJ. Dietary magnesium supplementation inhibits abdominal vascular calcification in an experimental animal model of chronic kidney disease. Nephrology, Dialysis, Transplantation: Official Publication of the European Dialysis and Transplant Association - European Renal Association. 2022; 37: 1049–1058. https://doi.org/10.1093/ndt/gfac026.

[18] He Q, Wen L, Wang L, Zhang Y, Yu W, Zhang F, *et al*. miR-15a-5p suppresses peritoneal fibrosis induced by peritoneal dialysis via targeting VEGF in rats. Renal Failure. 2020; 42: 932–943. https://doi.org/10.1080/0886022X.2020.1811123.

[19] Zareie M, De Vriese AS, Hekking LHP, ter Wee PM, Schalkwijk CG, Driesprong BAJ, *et al*. Immunopathological changes in a uraemic rat model for peritoneal dialysis. Nephrology, Dialysis, Transplantation: Official Publication of the European Dialysis and Transplant Association - European Renal Association. 2005; 20: 1350–1361. https://doi.org/10.1093/ndt/gfh835.

[20] Li P, Tao Z, Gao Y, Mu Z, Tian J, Zhang Y, *et al*. Ability of SPP1 to Alleviate Post-Intracerebral Hemorrhage Ferroptosis via Nrf2/HO1 Pathway. Brain and Behavior. 2025; 15: e70493. https://doi.org/10.1002/brb3.70493.

[21] Hu N, An R, Yu K, Chang Y, Gao W. PF4 induces inflammatory response through NF-kB signal pathway in rats with intracerebral haemorrhage. Folia Neuropathologica. 2023; 61: 379–386. https://doi.org/10.5114/fn.2023.130449.

[22] Zhang Z, Liu Y, Huang Q, Su Y, Zhang Y, Wang G, *et al*. NF-κB activation and cell death after intracerebral hemorrhage in patients. Neurological Sciences: Official Journal of the Italian Neurological Society and of the Italian Society of Clinical Neurophysiology. 2014; 35: 1097–1102. https://doi.org/10.1007/s10072-014-1657-0.

[23] Sozio SM, Armstrong PA, Coresh J, Jaar BG, Fink NE, Plantinga LC, *et al*. Cerebrovascular disease incidence, characteristics, and outcomes in patients initiating dialysis: The choices for healthy outcomes in caring for ESRD (CHOICE) study. American Journal of Kidney Diseases: The Official Journal of the National Kidney Foundation. 2009; 54: 468–477. https://doi.org/10.1053/j.ajkd.2009.01.261.

[24] Murray AM. Cognitive impairment in the aging dialysis and chronic kidney disease populations: an occult burden. Advances in Chronic Kidney Disease. 2008; 15: 123–132. https://doi.org/10.1053/j.ackd.2008.01.010.

[25] Li X, Jia R, Guo Y. Spontaneous brainstem haemorrhage in a

patient with uraemia undergoing initial hemodialysis: A case report. Experimental and Therapeutic Medicine. 2023; 25: 90. https://doi.org/10.3892/etm.2023.11789.

[26] Macellari F, Paciaroni M, Agnelli G, Caso V. Neuroimaging in intracerebral hemorrhage. Stroke. 2014; 45: 903–908. https://doi.org/10.1161/STROKEAHA.113.003701.

[27] Lei L, Qiao X, Siqi Y, Ke Y. Effects of Propofol Combined with Sufentanil Target-Controlled Intravenous Anesthesia on Expression of Bax, Bcl-2, and Caspase-3 Genes in Spontaneous Hypertensive Rats with Cerebral Hemorrhage: A Prospective Case-Controlled Study. Applied Biochemistry and Biotechnology. 2023; 195: 6068–6080. https://doi.org/10.1007/s12010-023-04378-0.

[28] Zhang Q, Wang L, Chen G, Wang M, Hu T. Cylindrospermopsin impairs vascular smooth muscle cells by P53-mediated apoptosis due to ROS overproduction. Toxicology Letters. 2021; 353: 83–92. https://doi.org/10.1016/j.toxlet.2021.10.006.

[29] Kang DH, Choi M, Chang S, Lee MY, Lee DJ, Choi K, *et al*. Vascular Proteomics Reveal Novel Proteins Involved in SMC Phenotypic Change: OLR1 as a SMC Receptor Regulating Proliferation and Inflammatory Response. PloS One. 2015; 10: e0133845. https://doi.org/10.1371/journal.pone.0133845.

[30] Nimmo AJ, Vink R. Recent patents in CNS drug discovery: The management of inflammation in the central nervous system. Recent Patents on CNS Drug Discovery. 2009; 4: 86–95. https://doi.org/10.2174/157488909788452997.

[31] Werner C, Engelhard K. Pathophysiology of traumatic brain injury. British Journal of Anaesthesia. 2007; 99: 4–9. https://doi.org/10.1093/bja/aem131.

[32] Tao J, Yang Z, Wang JM, Wang LC, Luo CF, Tang AL, *et al*. Shear stress increases Cu/Zn SOD activity and mRNA expression in human endothelial progenitor cells. Journal of Human Hypertension. 2007; 21: 353–358. https://doi.org/10.1038/sj.jhh.1002147.

[33] Landis GN, Tower J. Superoxide dismutase evolution and life span regulation. Mechanisms of Ageing and Development. 2005; 126: 365–379. https://doi.org/10.1016/j.mad.2004.08.012.

[34] Faraci FM, Didion SP. Vascular protection: Superoxide dismutase isoforms in the vessel wall. Arteriosclerosis, Thrombosis, and Vascular Biology. 2004; 24: 1367–1373. https://doi.org/10.1161/01.ATV.0000133604.20182.cf.

[35] Yada T, Shimokawa H, Hiramatsu O, Shinozaki Y, Mori H, Goto M, *et al*. Important role of endogenous hydrogen peroxide in pacing-induced metabolic coronary vasodilation in dogs in vivo. Journal of the American College of Cardiology. 2007; 50: 1272–1278. https://doi.org/10.1016/j.jacc.2007.05.039.

[36] Che Y, Zhang N, Zhu X, Li S, Wang S, Si H. Enhanced tolerance of the transgenic potato plants overexpressing Cu/Zn superoxide dismutase to low temperature. Scientia Horticulturae. 2020; 261: 108949. https://doi.org/10.1016/j.scienta.2019.108949.

[37] Satta S, Mahmoud AM, Wilkinson FL, Yvonne Alexander M, White SJ. The Role of Nrf2 in Cardiovascular Function and Disease. Oxidative Medicine and Cellular Longevity. 2017; 2017: 9237263. https://doi.org/10.1155/2017/9237263.

[38] Na HK, Surh YJ. Oncogenic potential of Nrf2 and its principal target protein heme oxygenase-1. Free Radical Biology & Medicine. 2014; 67: 353–365. https://doi.org/10.1016/j.freeradbiomed.2013.10.819.

[39] Gao MZ, Zeng JY, Chen XJ, Shi L, Hong FY, Lin M, *et al*. Dimethyl fumarate ameliorates oxidative stress-induced acute kidney injury after traumatic brain injury by activating Keap1-Nrf2/HO-1 signaling pathway. Heliyon. 2024; 10: e32377. https://doi.org/10.1016/j.heliyon.2024.e32377.

[40] Duan C, Wang H, Jiao D, Geng Y, Wu Q, Yan H, *et al*. Curcumin Restrains Oxidative Stress of After Intracerebral Hemorrhage in Rat by Activating the Nrf2/HO-1 Pathway. Frontiers in Pharmacology. 2022; 13: 889226. https://doi.org/10.3389/fphar.2022.889226.

[41] Preiser JC. Oxidative stress. JPEN. Journal of Parenteral and Enteral Nutrition. 2012; 36: 147–154. https://doi.org/10.1177/0148607111434963.

[42] Ozougwu JC. The role of reactive oxygen species and antioxidants in oxidative stress. International Journal of Research. 2016; 1: 1–8.

[43] Zhao P, Cao L, Wang X, Dong J, Zhang N, Li X, *et al*. Extracellular vesicles secreted by Giardia duodenalis regulate host cell innate immunity via TLR2 and NLRP3 inflammasome signaling pathways. PLoS Neglected Tropical Diseases. 2021; 15: e0009304. https://doi.org/10.1371/journal.pntd.0009304.

[44] Johnson JA, Johnson DA, Kraft AD, Calkins MJ, Jakel RJ, Vargas MR, *et al*. The Nrf2-ARE pathway: An indicator and modulator of oxidative stress in neurodegeneration. Annals of the New York Academy of Sciences. 2008; 1147: 61–69. https://doi.org/10.1196/annals.1427.036.

[45] Jadaun KS, Sharma A, Siddiqui EM, Mehan S. Targeting Abnormal PI3K/AKT/mTOR Signaling in Intracerebral Hemorrhage: A Systematic Review on Potential Drug Targets and Influences of Signaling Modulators on Other Neurological Disorders. Current Reviews in Clinical and Experimental Pharmacology. 2022; 17: 174–191. https://doi.org/10.2174/1574884716666210726110021.

[46] Shen X, Ma L, Dong W, Wu Q, Gao Y, Luo C, *et al*. Autophagy regulates intracerebral hemorrhage induced neural damage via apoptosis and NF-κB pathway. Neurochemistry International. 2016; 96: 100–112. https://doi.org/10.1016/j.neuint.2016.03.004.

[47] Yang Y, Tan X, Xu J, Wang T, Liang T, Xu X, *et al*. Luteolin alleviates neuroinflammation via downregulating the TLR4/TRAF6/NF-κB pathway after intracerebral hemorrhage. Biomedicine & Pharmacotherapy = Biomedecine & Pharmacotherapie. 2020; 126: 110044. https://doi.org/10.1016/j.biopha.2020.110044.